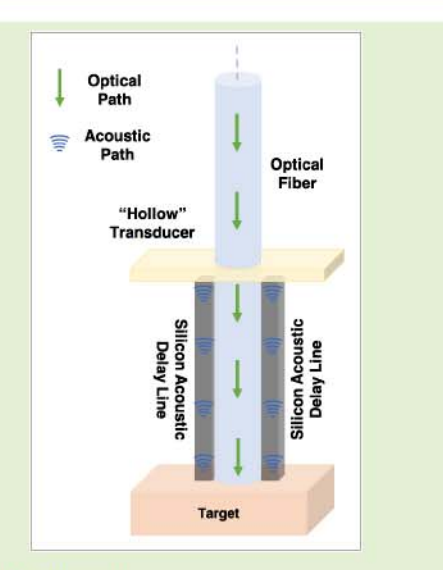


# A Photoacoustic Sensing Probe Based on Silicon Acoustic Delay Lines

Arif Kivanc Ustun<sup>®</sup>, Student Member, IEEE, and Jun Zou, Senior Member, IEEE

Abstract-In this paper, we report new photoacoustic sensing (PAS) probe design based on silicon acoustic delay lines (SADLs). It consists of an optical fiber for light delivery and two SADLs for detecting/relaying the generated PA signals to an outside receiving transducer. Ultrasound testing shows that acoustic signals can be transmitted along the SADLs with low loss up to 17~20 MHz. To improve the PA excitation efficiency, a beveled tip is formed at the distal end of the optical fiber to align the optical illumination region with the acoustic detection zone of the SADLs. New polymer micro linkers fabricated with high-resolution 3-D printing are used to maintain the mechanical stability and acoustic isolation within the probe assembly. For demonstration, a prototype SADL-PAS probe was designed and fabricated. Its PA sensing performance (e.g., sensitivity, linearity, and depth resolution) is characterized. Testing results show that the SADL-PAS probe provides superior sensitivity with considerable high-frequency improvement. Ex-vivo tests in the chicken breast are conducted to demonstrate the PA target detection in biological tissues.



Index Terms—Silicon acoustic delay lines, photoacoustic sensing, high frequency.

### I. INTRODUCTION

N RECENT years, photoacoustic sensing (PAS) probes [1]-[4] have been developed to conduct localized measurements in biological tissues. Different from conventional optical modalities, PAS can detect optical absorption contrast at a penetration depth beyond the optical diffraction limit [5]-[7]. However, the need for both light delivery and ultrasound detection poses some challenges in the design and construction of PAS probes, especially in terms of compactness. For *in-vivo* applications, the diameter of the sensing probe needs to be as small as possible to minimize its invasiveness. To achieve this, new PAS probe designs based on optical-fiber acoustic delay lines have been investigated [8], [9]. One or two optical fibers were used as both an optical waveguide for light delivery and an acoustic delay line for relaying the PA signal from the target to the receiving ultrasound transducer located outside of the probe shank. As a result, the overall diameter of the PAS probe can be significantly reduced. As an additional benefit, after transmitting through

Manuscript received July 2, 2021; revised August 2, 2021; accepted August 2, 2021. Date of publication August 11, 2021; date of current version October 1, 2021. This work was supported in part by the National Science Foundation under Award ECCS-1809710 and Award CMMI-1852184. The associate editor coordinating the review of this article and approving it for publication was Prof. Kea-Tiong Tang. (Corresponding author: Arif Kivanc Ustun.)

The authors are with the Department of Electrical and Computer Engineering, Texas A&M University, College Station, TX 77845 USA (e-mail: akustun87@tamu.edu; junzou@tamu.edu).

Digital Object Identifie 10.1109/JSEN.2021.3103932

the delay line, the PA signal will arrive at the transducer after all interference signals diminish and therefore can be easily distinguished and recorded for data processing. However, due to relatively low acoustic velocity (e.g., ~5000 m/sec [10]) of fused silica and also the acoustic attenuation within the optical fiber structure, the maximal single-mode acoustic transmission frequency of optical-fiber acoustic delay lines are typically limited to less than 5 MHz [2], [10]. As a result, the highfrequency components of the PA signal will be blocked. This situation not only limits the depth resolution of PA detection but can also reduce the detection sensitivity, because the peak amplitude of the PA signal oftentimes occurs at much higher frequencies (e.g., >10 MHz). To address this issue, we report a new PA sensing probe design based on silicon acoustic delay lines (SADLs). Compared with fused silica, single-crystalline silicon has much higher acoustic velocity (e.g., ~8000 m/sec [11], [12]) and lower acoustic attenuation. Therefore, it is possible to transmit the high-frequency components of the PA signals to improve both the depth resolution and sensitivity of PA detection. For demonstration, a prototype SADL-PAS probe was designed and fabricated. Its sensing performance was characterized within dye solutions with different concentrations, and biological tissues with an embedded optically-absorptive target.

### II. PROBE DESIGN AND CONSTRUCTION

Fig. 1a shows the schematic design of the SADL-PAS probe. The optical fiber for light delivery is located at the

1558-1748 © 2021 IEEE. Personal use is permitted, but republication/redistribution requires IEEE permission. See https://www.ieee.org/publications/rights/index.html for more information.

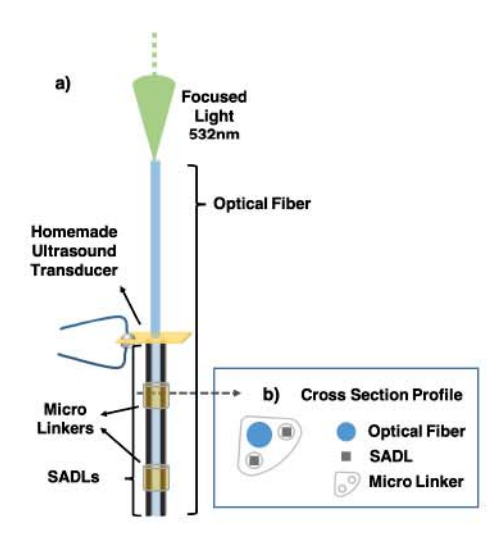


Fig. 1. Schematic design of the SADL-PAS probe.

center of the probe shank. Depending on the requirements on the PAS performance, a certain number of SADLs (surrounding the optical fiber) can be chosen for the detection of the PA signals. Their acoustic delay should be longer than the duration of the interference signals, such that the real PA signals from the target can be easily distinguished. Two or more micro linkers are used to hold the optical fiber and the SADLs in position while providing acoustic isolation between them. The "hollow" ultrasound transducer consists of a flat piezoelectric substrate with a drilled hole to allow the optical fiber to pass through. The diameter of the hole is slightly larger than that of the optical fiber, such that the ends of the surrounding SADLs can have good contact with the ultrasound transducer. Alternatively, an optically transparent transducer and two sections of optical fibers can be used [9]. However, the fabrication of the transparent transducer requires special piezoelectric substrate and electrode materials. Light coupling loss can also occur at the optical fiber and transducer interface. Therefore, the "hollow" transducer is more advantageous for the SADL-PAS probe design.

## A. Silicon Acoustic Delay Lines (SADLs)

To make the SADLs, silicon wires with a length of 25-mm and a cross-section of 100  $\mu$ m  $\times$  100  $\mu$ m were diced from a 4-inch 100-μm thick {100} silicon wafer. The 25-mm length of the SADLs gives an acoustic time delay of  $\sim 3 \mu s$  (assuming an acoustic velocity of 8400 m/s for silicon), which is longer than the typical duration of the interference signals during PA excitation [8]. For wire-type acoustic delay lines, the singlemode non-dispersive longitudinal transmission frequency is limited by its cross-sectional dimension [13]-[17], which is usually around 0.1 - 0.2c/d, where c and d are the acoustic velocity and the cross-sectional dimension of the delay line, respectively [18]. With a 100  $\mu$ m  $\times$  100  $\mu$ m cross-section, the highest single-mode transmission frequency of the SADLs is estimated to be  $\sim$ 17 MHz. Theoretically, a higher acoustic frequency range can be obtained by further shrinking the cross-sectional dimension of the SADLs. However, as the SADLs become thinner, they will have less reception area for

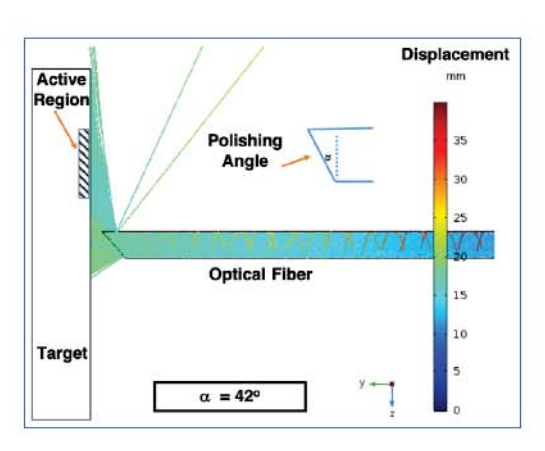


Fig. 2. Ray tracing simulation at a polishing angle of 42°.

PA signal detection and therefore lower sensitivity. Although this issue could be alleviated by increasing the number of the SADLs, their handling and assembly will become more difficult. In this work, two 100  $\mu$ m  $\times$  100  $\mu$ m SADLs are used as a trade-off in the construction of the prototype SADL-PAS probe. To minimize the probe diameter, the two SADLs are arranged on one side of the optical fiber for light delivery (Fig. 1b).

# B. Optical Fiber for Light Delivery

The optical fiber for light delivery is a fused-silica multimode optical fiber (FT200UMT, THORLABS, Newton, NJ) with a core diameter of 200  $\mu$ m, a clad layer of 12.5  $\mu$ m, and an overall diameter of 225  $\mu$ m. The 200- $\mu$ m core diameter allows the transmission of micro-joule ( $\mu$ J) laser pulses without damaging the fiber tip. Because the optical fiber and the SADLs are arranged side by side, this causes an offset of the light delivery and PA detection, resulting in lower PA detection efficiency [19], [20].

To improve the PA detection efficiency, the distal end of the fiber is polished at an oblique angle ( $\alpha$ ) to form a beveled tip to deflect a larger amount of light toward the center of the two SADLs. The beveled fiber tips were cut and polished by using a thin dicing blade at an oblique angle. A 3-D ray-tracing simulation was conducted with COMSOL Multiphysics® to determine the optimal polishing angle of the beveled tip in a cylinder-shape optical fiber. Fig. 2 shows the 2D view of the simulated rays on the cross-sectional plane of the incident optical fiber. As the polishing angle increases, more light beams from the optical fiber tip can be deflected to travel through the sidewall and illuminate the active detection region between the two SADLs for PA generation (Table. I). A significant portion of the deflected light for 34° and 42° illuminates the active region. To avoid any blockage, the beveled tip of the optical fiber needs to be extended by a certain distance beyond the SADLs. If the polishing angle is too big, the sharp tip will prevent good contact between the sensing target and SADLs for the detection of the PA signals. Therefore, a polishing angle of 42° was chosen as a good compromise.

### C. Micro Linkers

The optical fiber and two SADLs were held together with two micro linkers, which were fabricated with a

TABLE I
RAY TRACING SIMULATION RESULTS FOR
DIFFERENT OBLIQUE ANGLES

Polishing Angle (α)	Number of rays illuminating the A.R.* from its surface Total number of rays	
0°	0	
8°	0	
17°	0	
25°	0	
34°	0.065	
42°	0.122	

A.R.\*: Active Region

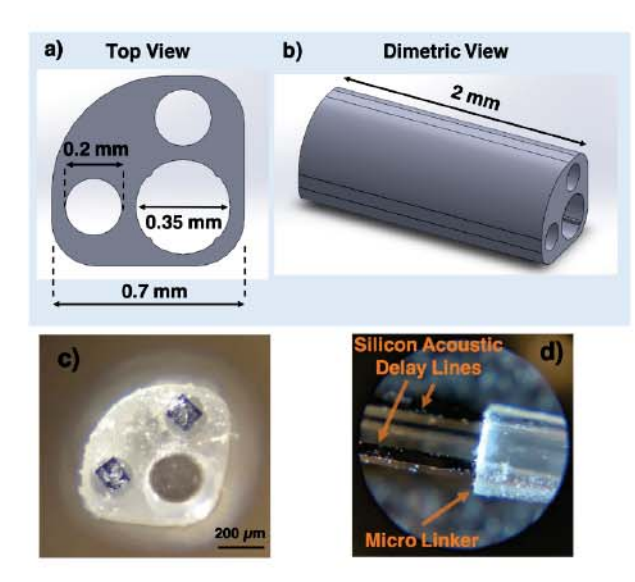


Fig. 3. Schematic design of the micro linker: a) End and b) Prospective view, and microscopic pictures of the assembly of two SADLs and a micro linker: c) End and d) Side view.

high-resolution 3D printer (Nanoscribe Photonics Professional GT2, Germany) at a spatial resolution (hatching and slicing distance) of 5  $\mu$ m (Fig. 3). The standard UV-curable (IP-Q) resin supplied by the manufacturer were used for the 3D printing, whose material properties are proprietary. The overall diameter and length of the micro linker are 700  $\mu$ m and 2 mm, respectively. To prevent acoustic leakage due to direct contact, the alignment holes for SADLs were formed into a circular shape with a diameter of 200  $\mu$ m to reduce the contact area between the micro linker and SADLs. The alignment hole for the optical fiber has a diameter of 350  $\mu$ m, which is slightly larger than that of the optical fiber (after the jacket layer is removed for space-saving). Four small protruding spacers were added to create a tiny gap between the optical fiber and the micro linker for further increasing the acoustic isolation. After the printing and development, the SADL holes had a diameter slightly smaller than the designed value and also relatively rough surface, possibly due to the low-resolution  $(5 \mu m)$  printing mode. After they were inserted into the micro linker, the SADLs were fixed in place by the friction without slipping.

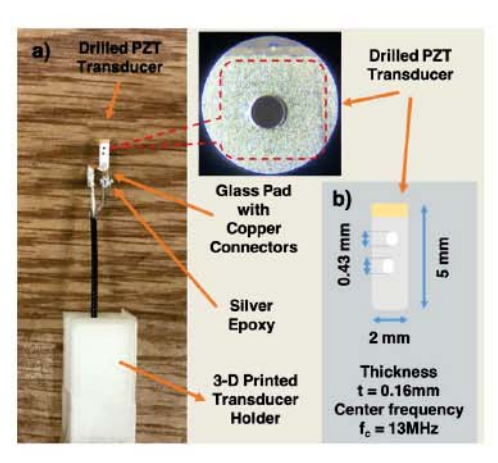


Fig. 4. a) Photo of transducer assembly and b) Illustration of drilled PZT substrate with detailed dimensions.

#### D. Ultrasound Transducer

To receive the PA signals through the SADLs, a home-made ultrasound transducer was fabricated on a 160- $\mu$ m-thick PZT (lead zirconate titanate) ceramic disc (Type VI, APC International Ltd., Mackeyville, PA), which has a thickness-mode resonance frequency of  $\sim$ 13 MHz (Fig. 4).

The PZT disc was diced into small pieces ( $5.0 \times 2.0 \text{ mm}^2$ ) to reduce the parasitic capacitance of the transducer. On the PZT disc, only the (small) region where the SADLs contact is the active region (for electrical charge generation) upon the reception of the PA signals. Other inactive regions of the PZT disc actually forms a parasitic capacitance, which reduces the effective output voltage of the transducer (as Vo = Q / ( $C_{active} + C_{parasitic}$ )). Therefore, the size of the PZT disc should be kept as small as possible to reduce the parasitic capacitance. On the other hand, it also needs to be large enough for wire connection.

A 430- $\mu$ m alignment hole and a spare hole were drilled to allow the optical fiber to pass through. Because the PZT disc operates in the thickness mode, the drilled hole is expected to have minimal effects on the overall performance of the transducer. To facilitate the wiring, two copper contact pads (one on the top and one on the bottom) were deposited onto the PZT substrate with e-beam evaporation. The PZT substrate was fixed onto a glass pad (also coated with two matching electrodes). Transducer mounting was completed by connecting the SMA connector to the glass-transducer assembly. No matching layer was added between the PZT transducer and the SADLs because the acoustic impedances of silicon and PZT are close to each other.

# III. TESTING AND CHARACTERIZATION A. Acoustic Transmission Through SADL

The acoustic transmission through a (bare) SADL was characterized with two-port ultrasound testing. The two-port ultrasound testing provides direct acoustic transmission information through the SADL, from which the acoustic velocity and bandwidth can be extracted. In addition, single-port (pulse-echo) ultrasound testing was also conducted on an SADL with or without micro linkers attached. The ultrasound signals transmitted by the transducer go through a round trip

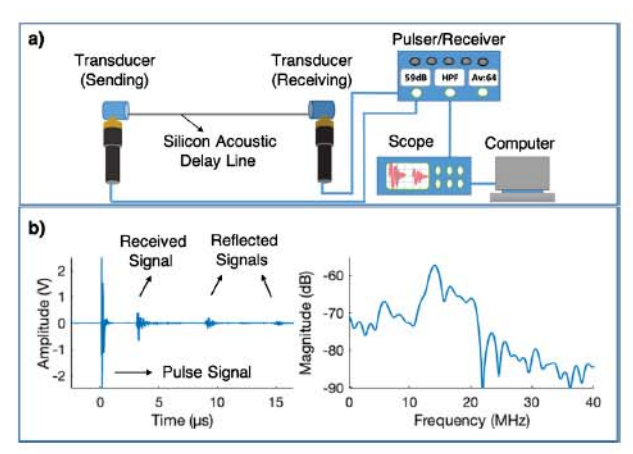


Fig. 5. Acoustic characterization of single SADL a) Two-port ultrasound testing setup and b) Time-domain ultrasound signals and their frequency spectra.

through the SADL before being received by the same transducer, which better manifests the possible acoustic attenuation and crosstalk caused by the micro linkers than a single trip.

In the two-port ultrasound testing, the SADL was placed between two 20-MHz ultrasound transducers (V250, Olympus NDT, Waltham, MA, USA) (Fig. 5a). Mineral oil was applied onto the contacts between the ends of acoustic delay fiber and the surfaces of transmitting & receiving transducers to enhance coupling efficiency and minimize unwanted reverberation. The pulser/receiver (5072PR, Olympus NDT, Waltham, MA) was set to the transmission mode, which sent a driving voltage pulse to the transmitting transducer to generate ultrasound signals and also amplified signals detected by a receiving transducer. Each received ultrasound signal was averaged 64 times and recorded on a digital oscilloscope (TDS2002C, Tektronix Inc., Beaverton, OR USA) to determine their peak amplitude and time delay.

Fig. 5b shows the received ultrasound signal after traveling through a SADL with a length of 25 mm. It arrived at the receiving transducer after a time delay is  $3.080~\mu s$ . The average acoustic velocity of SADLs is determined to be  $\sim 8120$  m/sec. The peak amplitude-frequency is around 14.2 MHz with 17% bandwidth. This result indicates that the coefficient of the single-mode transmission frequency (c/d) is close to 0.2.

In the single-port (pulse-echo) ultrasound testing, the SADL with two micro linkers assembled was contacted with one ultrasound transducer, which sent an ultrasound pulse into the SADL. After traveling along the SADL and reflected at both ends, the returning signals were detected by the same transducer (Fig. 6a). The ultrasound testing was repeated after two micro linkers were removed (Fig. 6b). In both cases, the attenuation of the ultrasound signals follows the same trend, which shows that the presence of the micro linker does not create significant attenuation in the acoustic transmission through the SADL (Fig. 6c and 6d). To determine the crosstalk, two-port ultrasound testing was conducted on two SADLs fixed by two micro linkers with the receiving transducer contacted with the same SADL (Fig. 6e), and the adjacent SADL (Fig. 6f), respectively. The received PA signal through the same SADL is arrived at the receiving

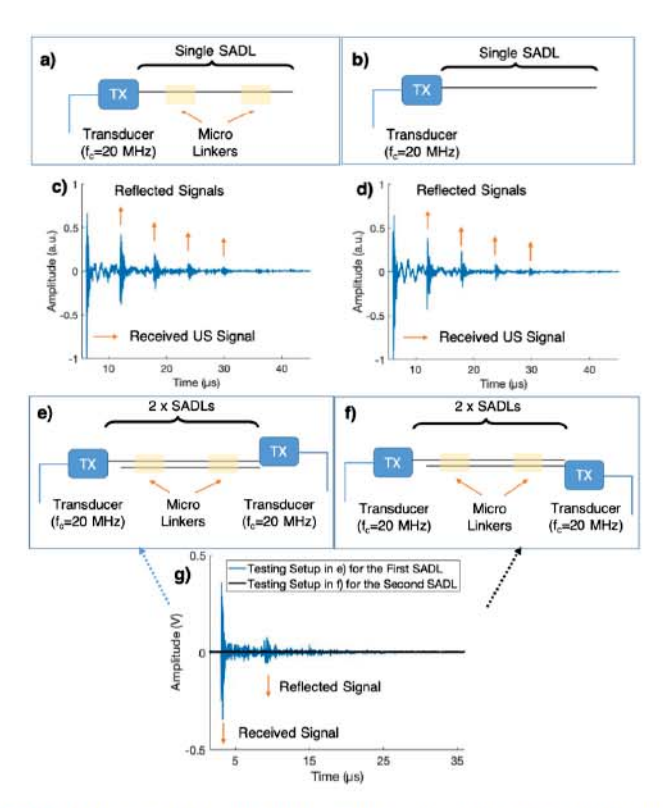


Fig. 6. Ultrasound characterization tests and results for the SADL-PAS probe structure: a) Pulse-echo ultrasound testing setup - single SADL with micro linkers, b) Pulse-echo ultrasound testing setup - single SADL without micro linkers, c) Results from the setup shown in a), d) Results from the setup shown in b). e) Acoustic transmission testing setup for two SADLs with two micro linkers (Receiving transducer contacted to the f rst SADL), f) Acoustic transmission testing setup for two SADLs with two micro linkers (Receiving transducer contacted to the second SADL), and g) Results from the setup shown in e) and f).

transducer after a delay of  $\sim 3~\mu s$ . The reflected signal has been obtained after  $\sim 9~\mu s$  as well (blue waveform in Fig. 6g). On the contrary, there is no noticeable signal detected when the receiving transducer has contacted with the second SADL (black waveform in Fig. 6g). These test results reveal that there is almost no acoustic crosstalk caused by the micro linkers.

## B. PA Characterization of the SADL-PAS Probe

The PA detection capability of the SADL-PAS probe was characterized with a test setup shown in Fig. 7a. The light source was an Nd:YAG laser (SPOT-10-200-532, Elforlight Ltd, Northants, UK) operating at a wavelength of 532 nm. The duration of the source pulse was 1.75 ns, and the maximum output energy was 20  $\mu$ J per pulse. The pulse repetition rate is 2 kHz. The probe assembly was supported by a 3D printed holder mounted on a three-axis stage (Fig. 7b). A black vinyl electrical tape serves as the target, which has a high optical absorption coefficient for efficient PA generation and strong internal acoustic damping with low reverberation. In this testing, the PAS probe was loosely contacted onto the surface of the black tape. To increase the acoustic coupling, a small amount of mineral oil was applied between the probe tip and the tape surface. The received PA signal was amplified and recorded on a digital oscilloscope with a sampling rate of 100 MHz.

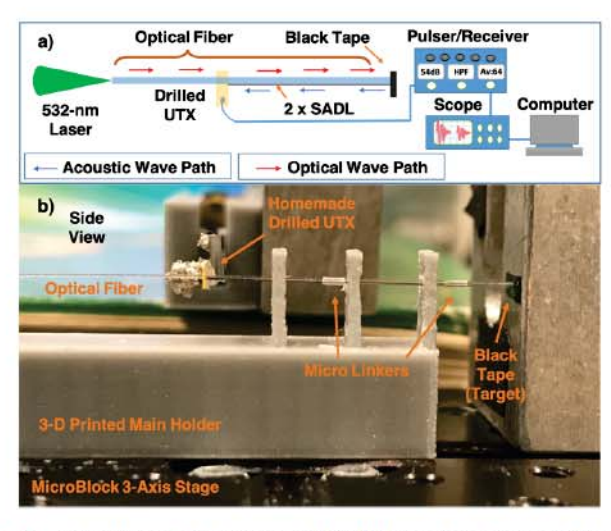


Fig. 7. PA testing setup for the SADL-PAS probe a) Schematic and b) Photo.

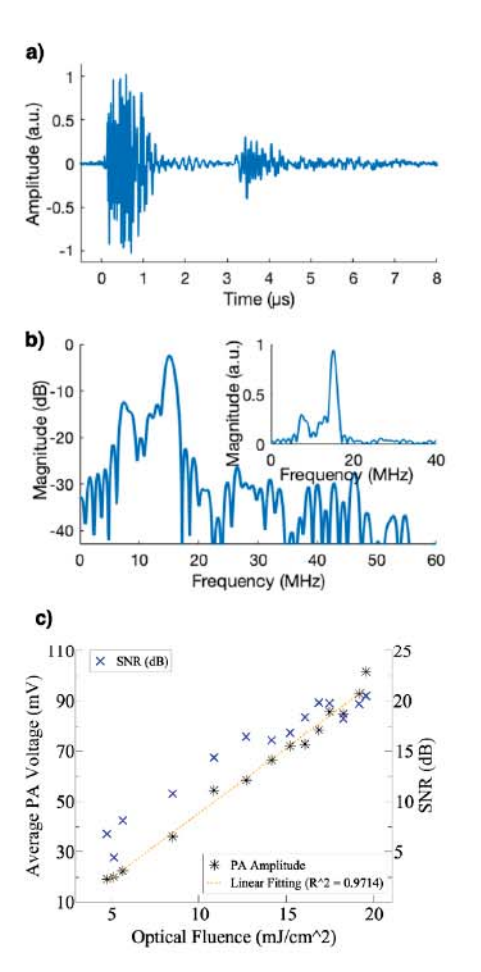


Fig. 8. a) Received time-domain PA signal, b) Frequency spectra of the PA signal, and c) Average PA voltage and SNR vs. Optical f uence.

Fig. 8a shows a received PA signal from the black tape target. It has a similar time delay and similar frequency spectrum (Fig. 8b) with that of the ultrasound signal (Fig. 5b). The acoustic bandwidth is slightly narrower, which is due to the smaller bandwidth of the home-made PZT transducer. For probe characterization, the laser power was set at different levels to reveal the relationship between the optical fluence and

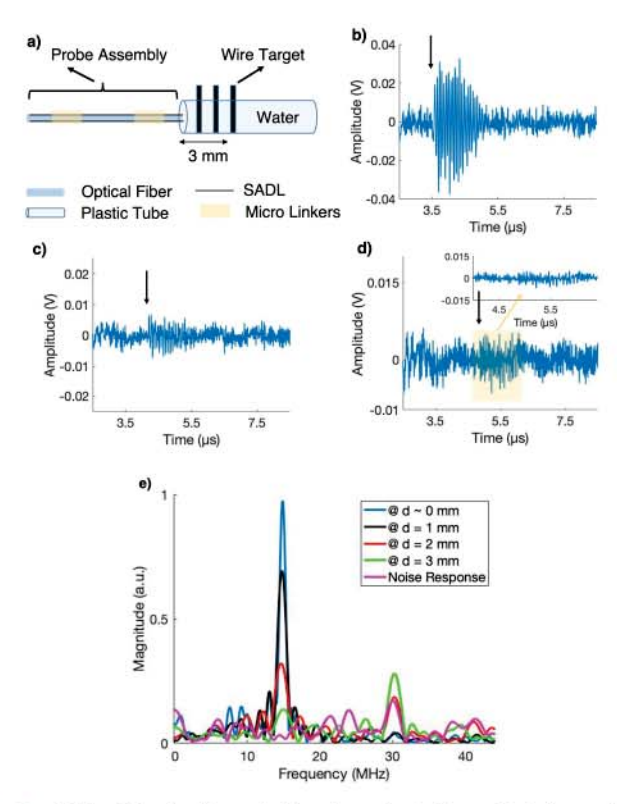


Fig. 9. PA test for depth resolution characterization: a) Testing setup, the received PA signals from the wire target located b) at 1 mm, c) at 2 mm, d) at 3 mm, and e) Frequency response of the PA signals.

the resulting PA signal strength (Fig. 8). The laser pulse energy and the optical fluence were determined based on the measured laser power, the pulse repetition rate, and also the estimated illumination area. At the probe tip, the maximal pulse energy was 7.77  $\mu$ J/pulse and the maximal optical fluence was 19.54 mJ/cm², which is below the ANSI (American National Standard Institute) safety limit of 20 mJ/cm² [21]. Both the PA voltage and SNR (signal-to-noise ratio) increases with the optical fluence. The PA voltage and the optical fluence follow a strong linear correlation (R² = 0.9714).

The PA characterization was repeated to characterize the depth resolution in a liquid solution. Compared with the PAS probes using optical fiber delay lines [8], [9], the ability to receive higher frequency components improves the temporal resolution of the PA signals and the resulting depth resolution of the target. A copper wire covered with a black plastic insulation layer was used as the target, which was placed at 1, 2, and 3 mm away from the probe tip, respectively (Fig. 9a). The target depths were estimated based on the time delay of the zero intersection of the received PA signals. The reference time delay was defined as the arrival time of the PA signal when the probe tip touches the copper wire (i.e., d = 0 mm) and only the time delay of the SADL is considered for the reference time delay. The amplitude of the PA received signal attenuates when the depth of the target increases from 1 mm to 3 mm (Figs .9b to .9d), due to lower optical fluence caused by stronger light diffusion at larger depths. After going deeper thicknesses than 3 mm, the PA signal started to be buried into noise, which indicates the maximal detection depth under the current testing condition. Acoustic time delays

TABLE II
ACOUSTIC TIME DELAY AND CALCULATED DEPTH OF THE TARGET

# Depth	Time Delay (µs)	Calculated Depth (mm)
0 mm	2.901	~ 0
1 mm	3.550	1.001
2 mm	4.197	1.997
3 mm	4.870	3.031

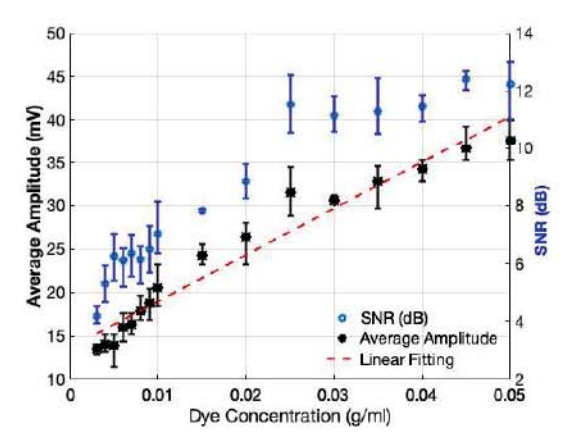


Fig. 10. PA signal amplitude and SNR from different black dye concentrations (g/ml).

at different depths (t) contain the combination of the time delay of the SADLs ( $\sim$ 2.900  $\mu$ s for this test) and that of water. Assuming an acoustic velocity of 1540 m/s in water, the nominal and calculated depths (based on time delay in water) are summarized in Table II. As shown in Fig. 9e, the peak frequency component of the PA signals occurs around 15 MHz, which matches with the results obtained in previous ultrasound and PA characterization (Fig. 5b and Fig. 8b). Based on the actual frequency spectra of the received PA signals and having completely noise components for the frequencies above 40 MHz, we have cropped out the signals above 40 MHz to generate a zoom-in view to show the details.

## C. Dye Concentration Characterization

The PA testing setup (Fig. 7) was also used for the dye concentration characterization. Dye solutions are prepared with black dye powder (Rit® Dye, Phoenix Brands, Stamford, CT) by diluting with deionized (DI) water to reach the desired concentration. For each dye concentration, five different PA tests were performed. A total of sixteen concentrations (n = 16) were tested ranging from 0.001 g/ml to 0.05 g/ml. The average PA peak voltage with the standard deviation is shown in Fig. 10. There exists a strong linear correlation between the peak PA voltage and dye concentration  $(R^2 = 0.934)$ . When the black dye concentration was reduced from 0.05 g/ml to 0.001 g/ml, the PA amplitude and SNR dropped from 39.2 mV to 8.2 mV and 13.78 dB to 2.36 dB, respectively. This result indicates a detection limit of about 0.001 g/ml, close to that obtained with the probes based on optical fiber delay lines (operating at a much lower frequency of  $2\sim3$  MHz) [2, 18]. The SNR is slightly lower (14 dB vs.

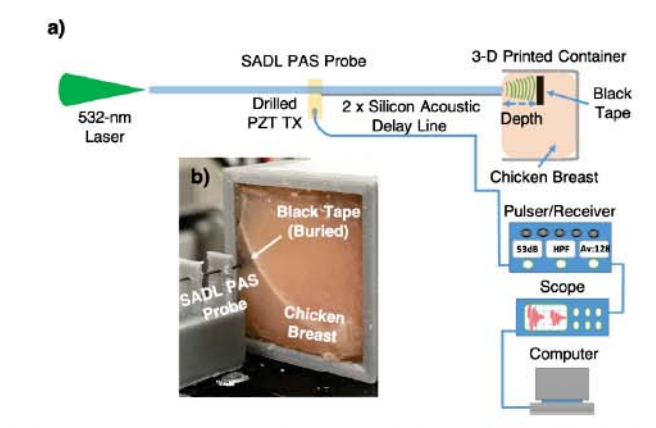


Fig. 11. PA test setup with chicken breast a) Diagram of the testing setup and b) Photo of the buried target and the top layer of chicken breast.

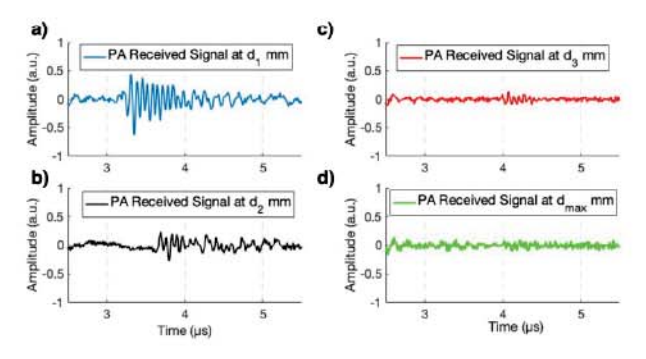


Fig. 12. Received PA signals from the black-tape target at different depths in chicken breast: a)  $d_1 = 0$ mm, b)  $d_2 = 0.8$ mm, c)  $d_3 = 1.34$ mm, and d)  $d_{max} = 1.51$ mm.

17∼18 dB), which could be due to two main factors. Firstly, the SADL has a much smaller cross-section (for PA signal reception) than the optical fibers. Secondly, the sensitivity of the ultrasound transducers is inversely related to their operating frequencies. Therefore, a lower PA detection sensitivity would be expected from the SADL-PAS probe with much higher detection frequencies.

### IV. TARGET DETECTION IN BIOLOGICAL TISSUES

The capability of the SADL-PAS probe for PA detection in biological tissues is demonstrated by utilizing chicken breast as the testing medium (Fig. 11a). A 3-D printed container held two layers of chicken breast tissue in place. One-layer was laid in the container first. The target (a piece of black tape) was placed onto this first layer and the second layer topped the target, whose thickness (0.8 mm, 1.3 mm, and 1.5 mm) defines the depth of the target (Fig. 11b). To acquire the PA signal, the tip of the SADL-PAS probe was aligned to the black-tape target and slowly contacted onto the surface of the second layer of chicken breast. Fig. 12 shows the PA signals from the black tape target at different depths of the second layer of the chicken breast. These depths were  $d_1 = 0$  mm,  $d_2 = 0.8 \text{ mm}, d_3 = 1.34 \text{ mm}, \text{ and } d_{\text{max}} = 1.51 \text{ mm}.$  Based on the acoustic velocity of 1540 m/s in chicken breast [22], the target depths were estimated based on the time delay of the zero intersection of the PA signals, which is similarly obtained in Fig. 9. After going deeper thicknesses than d<sub>max</sub>, the PA signal started to be buried into noise. The reduced detection depth is mainly due to the (much) higher optical scattering and also increased acoustic attenuation in the chicken breast tissue.

### V. CONCLUSION AND DISCUSSION

In conclusion, a new SADL-PAS probe design has been demonstrated with a few innovative features. First, the SADLs allow the transmission of higher-frequency components of the PA signals, which are received by a "hollow" transducer without blocking the optical path. Second, specially designed 3-D micro linkers keep the SADLs and optical fiber in place within a compact probe structure, while creating little acoustic attenuation and crosstalk. Third, with a beveled fiber tip, the optical illumination and the acoustic detection regions overlap with each other, which helps to improve the PA generation efficiency and detection sensitivity. The sensing performance of the SADL-PAS probe has been characterized by different targets. Experimental results show that the SADL-PAS probe has good sensitivity, linearity, and superior high-frequency response over those based on optical fiber delay lines.

Theoretically, a higher PA detection frequency range can be obtained by further shrinking the cross-section of the SADLs, which however will reduce both the mechanical strength and the acoustic detection sensitivity. This issue can be alleviated by increasing the number of SADLs. Nevertheless, as the SADLs become thinner and more fragile, their handling and assembly will be more challenging. To address this issue, a new integrative micromachining process would be needed to minimize or eliminate the (manual) assembly steps. In addition, the PA signals are usually wide-band signals. A backing layer can be added onto the transducer to increase its bandwidth, which is expected to further improve the depth resolution of the PA detection.

In addition to single point sensing, the SADL-PAS probe can be used to conduct high-resolution photoacoustic tomography without expensive high-frequency transducer arrays. When multiple probes with different delay times are bundled into an array, the PA signals will reach one common (single-element) transducer at different times and therefore can be received unambiguously in a time-serial manner with just one data acquisition channel. 2D or 3D image reconstruction can be performed based on the received PA signals.

# REFERENCES

- W. Xia et al., "Fiber optic photoacoustic probe with ultrasonic tracking for guiding minimally invasive procedures," in Proc. Eur. Conf. Biomed. Opt. Washington, DC, USA: Optical Society of America, 2015, Art. no. 95390K.
- [2] Y. Cho et al., "Handheld photoacoustic tomography probe built using optical-fiber parallel acoustic delay lines," J. Biomed. Opt., vol. 19, no. 8, Aug. 2014, Art. no. 086007.
- [3] C. Kim et al., "Handheld array-based photoacoustic probe for guiding needle biopsy of sentinel lymph nodes," Proc. SPIE, vol. 15, no. 4, 2010, Art. no. 046010.
- [4] C. Kim, T. N. Erpelding, L. Jankovic, and L. V. Wang, "Performance benchmarks of an array-based hand-held photoacoustic probe adapted from a clinical ultrasound system for non-invasive sentinel lymph node imaging," *Philos. Trans. Roy. Soc. London A, Math. Phys. Sci.*, vol. 369, no. 1955, pp. 4644–4650, 2011.

- [5] L. V. Wang, "Prospects of photoacoustic tomography," Med. Phys., vol. 35, no. 12, pp. 5758–5767, Nov. 2008.
- [6] V. Ntziachristos, "Going deeper than microscopy: The optical imaging frontier in biology," *Nature Methods*, vol. 7, no. 8, pp. 603–614, 2010.
- [7] P. Beard, "Biomedical photoacoustic imaging," *Interface Focus*, vol. 1, no. 4, pp. 602–631, 2011.
- [8] A. K. Ustun and J. Zou, "A photoacoustic sensing probe using optical fiber acoustic delay line," *Photoacoustics*, vol. 13, pp. 18–24, Mar. 2019.
- [9] A. K. Ustun and J. Zou, "A photoacoustic sensing probe using single optical fiber acoustic delay line," *IEEE Sensors J.*, vol. 19, no. 19, pp. 8714–8719, Oct. 2019.
- [10] I. L. Gelles, "Optical-fiber ultrasonic delay lines," J. Acoust. Soc. Amer., vol. 39, no. 6, pp. 1111–1119, Jun. 1966.
- [11] B. A. Auld, Acoustic Fields and Waves in Solids. Moscow, Russia: Ripol Classic, 1973.
- [12] J. D. N. Cheeke, Fundamentals and Applications of Ultrasonic Waves. Boca Raton, FL, USA: CRC Press, 2017.
- [13] J. E. May, "Wire-type dispersive ultrasonic delay lines," IRE Trans. Ultrason. Eng., vol. 7, no. 2, pp. 44–52, 1960.
- [14] T. R. Meeker, "Dispersive ultrasonic delay lines using the first longitudinal mode in a strip," *IRE Trans. Ultrason. Eng.*, vol. 7, no. 2, pp. 53–58, Jun. 1960.
- [15] A. H. Meitzler, "Ultrasonic delay lines for digital data storage," IRE Trans. Ultrason. Eng., vol. 9, no. 2, pp. 30–37, 1962.
- [16] J. H. Eveleth, "A survey of ultrasonic delay lines operating below 100 Mc/s," Proc. IEEE, vol. 53, no. 10, pp. 1406-1428, Oct. 1965.
- [17] T. Moriya, Z. Hu, and Y. Tanahashi, "Development of flexible acoustic transmission line for intravascular ultrasonography," in *Proc. IEEE Ultrason. Symp. Int. Symp.*, vol. 2, Oct. 2000, pp. 1227–1230.
- [18] M. K. Yapici et al., "Parallel acoustic delay lines for photoacoustic tomography," J. Biomed. Opt., vol. 17, no. 11, Nov. 2012, Art. no. 116019.
- [19] E. M. Strohm, M. J. Moore, and M. C. Kolios, "Single cell photoacoustic microscopy: A review," *IEEE J. Sel. Topics Quantum Electron.*, vol. 22, no. 3, pp. 137–151, May 2016.
- [20] T. Zhao, A. E. Desjardins, S. Ourselin, T. Vercauteren, and W. Xia, "Minimally invasive photoacoustic imaging: Current status and future perspectives," *Photoacoustics*, vol. 16, Dec. 2019, Art. no. 100146.
- [21] American National Standard for the Safe Use of Lasers, Standard ANSI Z136. American National Standards Institute, New York, NY, USA, 2007.
- [22] A. Sarvazyan and S. Tsyuryupa, "Potential biomedical applications of non-dissipative acoustic radiation force," in *Proc. Meetings Acoust.* Melville, NY, USA: Acoustical Society of America, 2016, vol. 26, no. 1, Art. no. 020002.



Arif Kivanc Ustun (Student Member, IEEE) received the B.Sc. degree from Anadolu University, Turkey, in 2009, and the M.Eng. and Ph.D. degrees from Texas A&M University in 2014 and 2021, respectively. His current research interests include micro-electro-mechanical systems (MEMS), acoustic delay lines, novel photoacoustic and ultrasound medical systems, and relevant micro-nano fabrication methods. He is a Student Member of SPIE.



Jun Zou (Senior Member, IEEE) received the Ph.D. degree in electrical engineering from the University of Illinois at Urbana–Champaign in 2002. He joined the Department of Electrical and Computer Engineering, Texas A&M University, in 2004, where he is currently a Full Professor. His current research interests include the development of micro and nano opto-electromechanical devices and systems for biomedical imaging and sensing applications. He is a Senior Member of SPIE and a member of OSA.